AD-A066 100 TRW DEFENSE AND SPACE SYSTEMS GROUP REDONDO BEACH CALIF F/G 18/6
MCCABE: A CODE FOR CALCULATING X-RAY INDUCED CURRENTS IN SHIELD--ETC(U)
FEB 78 D M CLEMENT, C E WULLER DNA001-77-C-0084

UNCLASSIFIED DNA-4541F NL

| OF |

AD
A066100

END
DATE
FILMED
5-79
DDC

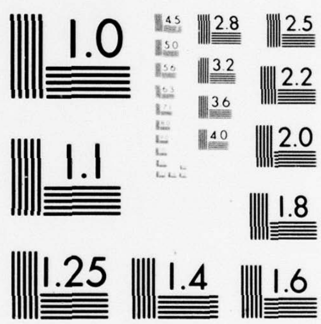
1.0
1.1
1.25
1.4
1.6
1.8
2.0
2.2
2.5
2.8
3.2
3.6
4.0
4.5
5.0
5.6

AD-E300 457

(12) LEVEL III

DNA 4541F

AD A0 66100

MCCABE: A CODE FOR CALCULATING X-RAY INDUCED CURRENTS IN SHIELDED CABLES

TRW Defense & Space Systems Group
One Space Park
Redondo Beach, California 90278

28 February 1978

Final Report for Period May 1977—December 1977

CONTRACT No. DNA 001-77-C-0084

APPROVED FOR PUBLIC RELEASE;
DISTRIBUTION UNLIMITED.

THIS WORK SPONSORED BY THE DEFENSE NUCLEAR AGENCY
UNDER RDT&E RMSS CODE B323077464 R99QAXEE50307 H2590D.

Prepared for
Director
DEFENSE NUCLEAR AGENCY
Washington, D. C. 20305

Destroy this report when it is no longer needed. Do not return to sender.

PLEASE NOTIFY THE DEFENSE NUCLEAR AGENCY, ATTN: TISI, WASHINGTON, D.C. 20305, IF YOUR ADDRESS IS INCORRECT, IF YOU WISH TO BE DELETED FROM THE DISTRIBUTION LIST, OR IF THE ADDRESSEE IS NO LONGER EMPLOYED BY YOUR ORGANIZATION.

UNCLASSIFIED

SECURITY CLASSIFICATION OF THIS PAGE (When Data Entered)

REPORT DOCUMENTATION PAGE		READ INSTRUCTIONS BEFORE COMPLETING FORM
1. REPORT NUMBER DNA 4541F	2. GOVT ACCESSION NO.	3. RECIPIENT'S CATALOG NUMBER
4. TITLE (and Subtitle) MCCABE: A CODE FOR CALCULATING X-RAY INDUCED CURRENTS IN SHIELDED CABLES		5. TYPE OF REPORT & PERIOD COVERED Final Report for Period May 1977—December 1977
		6. PERFORMING ORG. REPORT NUMBER
7. AUTHOR(s) David M. Clement Charles E. Wuller		8. CONTRACT OR GRANT NUMBER(s) DNA 001-77-C-0084
9. PERFORMING ORGANIZATION NAME AND ADDRESS TRW Defense and Space Systems Group One Space Park Redondo Beach, California 90278		10. PROGRAM ELEMENT, PROJECT, TASK AREA & WORK UNIT NUMBERS Subtask R99QAXEE503-07
11. CONTROLLING OFFICE NAME AND ADDRESS Director Defense Nuclear Agency Washington, D.C. 20305		12. REPORT DATE 28 February 1978
		13. NUMBER OF PAGES 46
14. MONITORING AGENCY NAME & ADDRESS(if different from Controlling Office) 12 45p.		15. SECURITY CLASS (of this report) UNCLASSIFIED
		15a. DECLASSIFICATION DOWNGRADING SCHEDULE

16. DISTRIBUTION STATEMENT (of this Report)

Approved for public release; distribution unlimited.

18 DNA, SBIE 19 4541F, AD-E300 457

17. DISTRIBUTION STATEMENT (of the abstract entered in Block 20, if different from Report)

18. SUPPLEMENTARY NOTES

This work sponsored by the Defense Nuclear Agency under RDT&E RMSS Code B323077464 R99QAXEE50307 H2590D.

19. KEY WORDS (Continue on reverse side if necessary and identify by block number)

Cables
X-Ray Response
(Multi-Conductor Cable),

20. ABSTRACT (Continue on reverse side if necessary and identify by block number)

The theory and operation of MCCABE, a code for calculating X-ray induced currents in shielded cables, is described. The code is applicable to cables in vacuum where the incident X-ray flux is low enough that radiation induced conductivity and other limiting effects may be ignored.

DD FORM 1 JAN 73 1473 EDITION OF 1 NOV 65 IS OBSOLETE

UNCLASSIFIED

SECURITY CLASSIFICATION OF THIS PAGE (When Data Entered)

409637 79 01 26 010

TABLE OF CONTENTS

LIST OF FIGURES

LIST OF TABLES

1.0 INTRODUCTION

This report summarizes the theory and operation of the MCCABE (Multi-Conductor-CABlE code) which is an analytical tool for predicting the response of shielded cables or cable bundles in X-ray environments, and is a multi-conductor generalization of the PICS code reported in Ref. 9. The output of the MCCABE code is the per-unit-length eqivalent circuit parameters for transmission lines, chief among which is the radiation driven current source terms. The underlying assumptions and limitations of the code are discussed in Sect.2, but the main assumptions are that:

1) the cables are in vacuum;
2) the incident flux is low enough such that radiation induced conductivity and other limiting effects may be ignored;
3) there is no significant x-ray spectral content above 300 keV.

The MCCABE formalism presented in Sect. 2 differs from that in Ref. 1 in that the electron transport routines have been completely revised to use the analytic charge deposition profile analysis recently given by Dellin and MacCallum.[4] The advantage of their deposition profile results (besides computing speed) is that electron production from both materials which form an interface (e.g. conductor and dielectric) is automatically taken into account. The MCCABE code can now calculate the response of a cable made from materials with comparable emission efficiencies (e.g. aluminum and Kel-F).

The operation of the code is discussed in Sect. 3 where sample input and output are also presented. One important feature of the code is an executive subprogram which interrogates the user concerning the input to the code (cable dimensions, materials, etc.). This subprogram sets up all the input files for the problem, and the user doesn't have to concern himself about format. The running time for a coax problem is less than 12 sec CPU time on the CDC 6600, with multi-conductor cables taking longer.

The MCCABE code has been used recently in a parameter study[2)] to determine the sensitivity of cable response to various cable and photon source parameters. Before running the MCCABE code we suggest that the user consult Ref. 2 in order to get a rough idea of how his cable will respond.

At this point the MCCABE code has received preliminary experimental verification in X-radiation experiments conducted at the Simulation Physics facilities[7,8] and the Aerospace Dense Plasma Focus facility[7,9]. References 7-9 concerned either coaxial cable response, or common-mode multi-conductor cable response; Reference 1 considered individual wire response of multi-conductor cable response as well. The fluence at both the SPI and DPF machines was on the order of 10^{-4} to 10^{-3} cal/cm^2. An experimental program for testing cables is presently underway at the SPI facilities, and will be reported later.

As mentioned above, the code is applicable to the region where radiation induced conductivity and other limiting effects are unimportant. We believe that the cross-over point occurs at a few tenths of a cal/cm^2, and that beyond this the response is sublinear. This point is discussed in more detail in Ref. 3. The implication is that MCCABE can still provide worst-case estimates of cable response even at high fluences.

2.0 THEORY OF THE MCCABE CODE

The problem of determining the response of shielded cables to x-rays can be considered in three steps:

Step 1: Calculation of the photon transport, electron production and transport for the geometry and materials of the cable to determine the profile of deposited charge in cable dielectrics;

Step 2: Calculation of the radiation driven source terms (Norton equivalent drivers) to be used in the transmission line equations.

Step 3: Solution of the transmission line equations to obtain load response.

The MCCABE code carries out the first two steps, again assuming that no limiting occurs and that the radiation transport is independent of any voltages developed along the transmission line. With these assumptions the Norton driver can be inserted into transmission line equations in a separate step. On the other hand, if limiting effects are important, then steps 2 and 3 are coupled and must be solved simultaneously.

In the subsections below we discuss the following topics:

- transmission line equations and equivalent circuit modeling (Sect. 2.1)
- cable geometry and photon attenutation (Sect. 2.2)
- electron deposition in cables (Sect. 2.3)
- the solution of Laplace's equation in two dimensions (Sect. 2.4)

2.1 TRANSMISSION LINE EQUATIONS AND EQUIVALENT CIRCUIT MODEL

We derive the canonical transmission line equations which include the desired X-ray induced source terms. The key assumption of transmission line theory is that only the TEM mode of propagation is important, and this implies that the electromagnetic fields are normal to the axis of propagation. An immediate consequence of this is that the electric field is derivable from a scalar potential.

Differential Voltage Transmission Line Equation:

Consider N wires inside a shield, as in Fig. 2.1.1. Consider the magnetic flux linked between the i^{th} conductor and the shield which is taken as reference. From Lenz's law we have

$$\oint_c \vec{E} \cdot d\vec{\ell} = -\frac{d}{dt} \int \vec{B} \cdot d\vec{A} \ . \tag{2.1.1}$$

The contour integration is defined in Fig. 2.1.1. If $\vec{J}$, the photo Compton current density, is uniform, and normal to the conductor axes, the net flux linked by $\vec{J}$ is zero, and only the propagation current along the wires, I_i, contributes to the flux. By definition, each of these will make a contribution to the magnetic flux by an amount $L_{ij} I_j \Delta z$, where L_{ij} is the mutual inductance per unit length of the wires i and j, and L_{ii} is the self-inductance per unit length of the i^{th} wire. Since $\vec{E}$ is normal to the conductor axis and is also derivable from a scalar potential, the LHS is just

$$V_i + \Delta V_i - V_i \simeq \frac{\partial V_i}{\partial z} \Delta z \ , \tag{2.1.2}$$

where V_i is the potential of the i^{th} wire with respect to reference, and we obtain the first transmission line equation,

$$\frac{\partial V_i}{\partial z} = -\sum_j L_{ij} \frac{\partial I_j}{\partial t} \ . \tag{2.1.3}$$

Differential Current Transmission Line Equation:

From potential theory the total charge per unit length Q_i on conductor i is given by

$$\underbrace{Q_i}_{\substack{\text{total charge}\\ \text{per unit length}}} = \underbrace{-\int d^2r \, q(\vec{r})\psi_i(\vec{r})}_{\substack{\text{induced charge}\\ \text{per unit length}}} + \underbrace{\sum_{j=1}^{N} k_{ij} V_j}_{\substack{\text{capacitive charge}\\ \text{per unit length}}} \ . \tag{2.1.4}$$

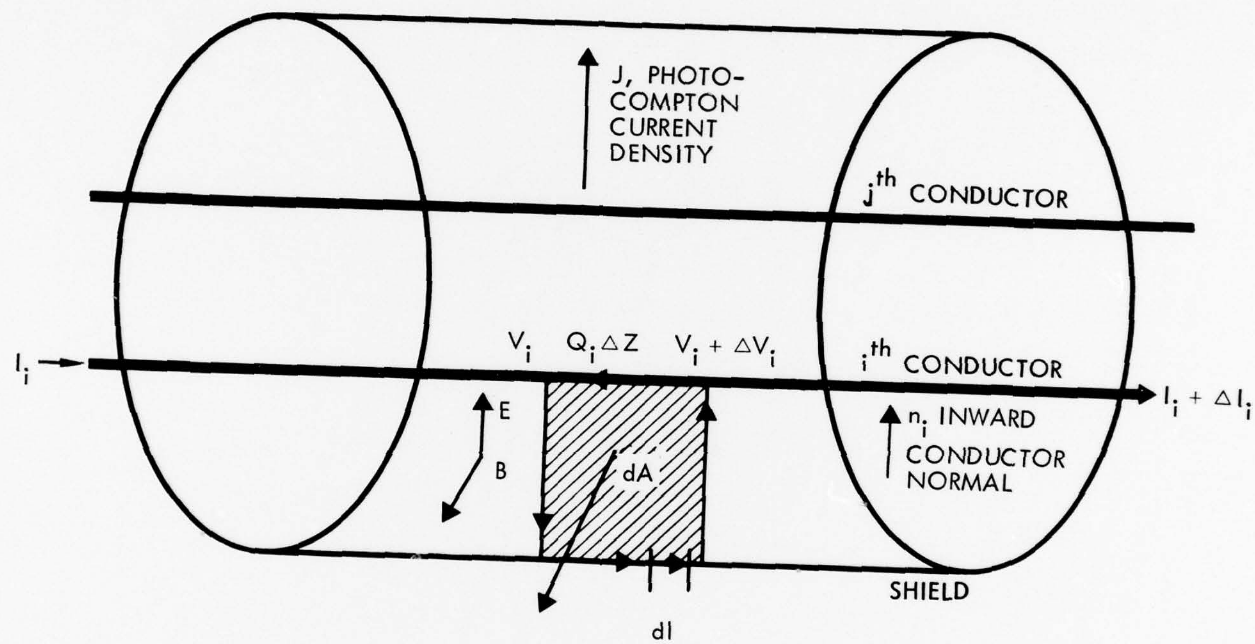

Figure 2.1.1 Derivation of the transmission line equations including radiation-driven source terms.

(This expression is derived in Appendix A). Here q is the volume charge density at any instant of time, $\psi_i(\vec{r})$ is a solution of Laplace's equation with unit potential on conductor i, and zero on the rest. The k_{ij} are the elements of Maxwell's capacitance matrix, and are obtained by placing a unit potential on each conductor j, grounding the rest, solving Laplace's equation, and obtaining the induced charge. Then $Q_i \equiv k_{ij}$.

Now, the rate at which charge is deposited in the element Δz on conductor i, is simply the difference between the incoming current $I_i(z)$ and the outgoing current $I_i\,(z+\Delta z)$, or simply $-(\partial I/\partial z)\Delta z$. This is equal to the sum of two terms: (1) $(\partial Q_i/\partial t)\Delta z$, which includes both induced and capacitive charge (Eq. 2.1.4), and also (2) the rate of direct charge arrival, $\Delta z \oint_{c_i} dl_i\, \vec{J}\cdot\vec{n}_i$, where $\vec{n}_i$ is the surface normal directed <u>into</u> the conductor. The result of this is the second transmission line equation

$$\frac{\partial I_i}{\partial z} = K_i - \sum_{j=1}^{N} k_{ij} \frac{\partial V_j}{\partial t} \quad , \tag{2.1.5}$$

where the source term (i.e., the Norton equivalent current driver) is given by

$$K_i = \int d^2r \frac{\partial q}{\partial t} \psi_i\,(\vec{r}) - \oint_{c_i} dl_i\, \vec{J}\cdot\vec{n}_i \quad , \tag{2.1.6}$$

and $\partial q/\partial t$ is related to the photo-Compton current via the continuity equation

$$\frac{\partial q}{\partial t} = - \vec{\nabla} \cdot \vec{J} \ . \tag{2.1.7}$$

By construction $\vec{J}$ only includes the photo-Compton current, though in principle a conductivity term could be added. Since we have assumed that both $\vec{J}$ and $\partial q/\partial t$ follow the radiation pulse, then so do the K_i.

The transmission line equations (2.1.3) and (2.1.5) may be solved directly, of course, but if conventional circuit analysis codes are to be used, then the equivalent circuit lumped elements of a section of transmission line of length Δz are shown in Fig. 2.1.2. If N is the total number of inner wires, the model consists of N current drivers $K_i\Delta z$, $N(N+1)/2$ capacitances $C_{ij}\Delta z$, and twice that many self-and mutual inductances $1/2L_{ij}\Delta z$. The elements of Maxwell's capacitance matrix k_{ij} are related to empirical capacitances C_{ij} in Fig. 2.1.2 by the relations

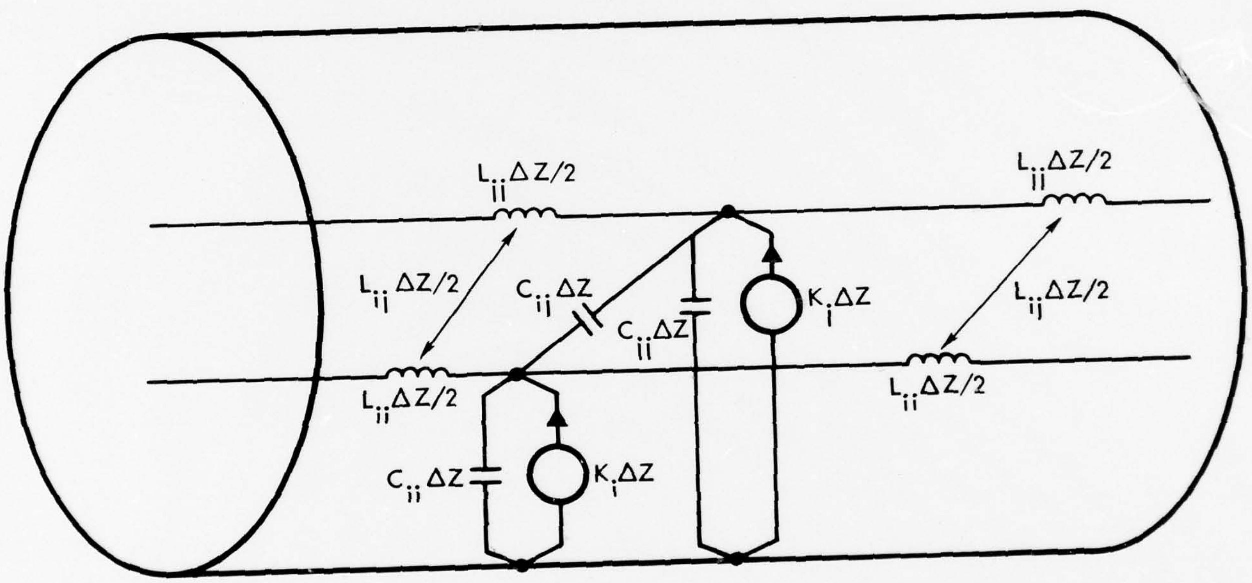

Figure 2.1.2 Equivalent circuit model for a multi-conductor transmission line including radiation induced source terms.

$$C_{ij} = -k_{ij},\ i \neq j,$$

$$C_{ii} = \sum_{j'}^{N} k_{ij'}\ ,\ i=j\ . \qquad (2.1.8)$$

If the assumption of lossless lines and homogeneous dielectrics is made, then the self and mutual inductances may be obtained by solving the equations

$$\sum_{j=1}^{N} L_{ij} k_{j\ell} = \delta_{i\ell}\, v^{-2}$$

where v is the velocity of propagation along the cable axis.

2.2 MULTICONDUCTOR CABLE GEOMETRY AND PHOTON ATTENUATION

Next, we discuss the details of the incident photon spectrum. Throughout this work we are assuming that there is no time delay in electron-photon transport and that the current drivers, which are the output of this code, are proportional to the instantaneous photon flux. With this in mind the user specifies the instantaneous photon flux $\dot{F}$ and an energy spectrum. For convenience this could be the peak flux associated with a given pulse. Then when subsequent transmission line codes are driven by the Norton equivalent drivers

$$\text{Norton driver} = \text{peak Norton driver} \times \text{pulse envelope}$$

where the "pulse envelope" is just the pulse waveform normalized to unity at the peak of the pulse. In addition all results scale with flux, so any convenient unit of flux is appropriate.

The source may have either an arbitrary unnormalized photon energy distribution U(E) or a blackbody distribution of the form

$$U(E) \equiv \frac{E^3}{\exp(E/kT) - 1} \, . \tag{2.2.1}$$

Suppose a distribution such as that shown in Fig. 2.2.1 were given.

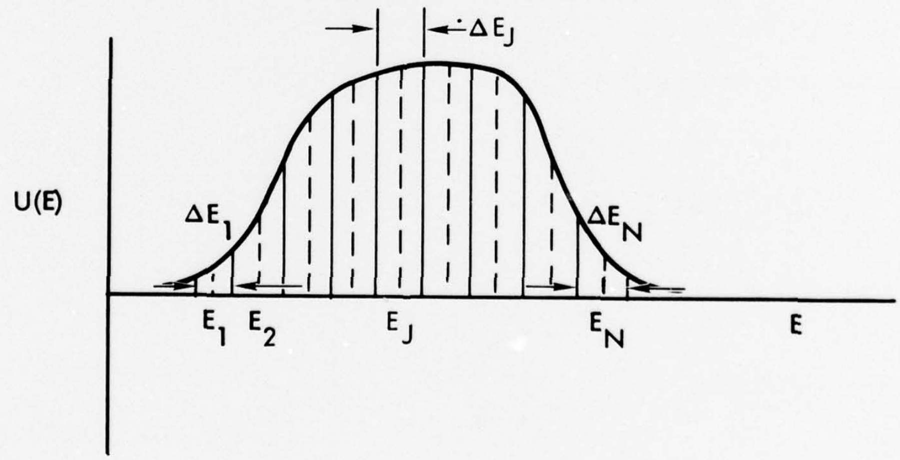

Figure 2.2.1 Unnormalized photon energy distribution.

One proceeds to discretize the spectrum by picking out photon energies E_j (the dashed lines in the figure) which are not necessarily uniformly spaced. Then the total un-normalized energy flux would be approximated by

$$\int U(E)\, dE \approx \sum_{j=1}^{N} U(E_j)\, \Delta E_j \ , \tag{2.2.2}$$

$$\Delta E_j \equiv \begin{cases} E_2 - E_1 \ , \ j = 1 \ , \\ \frac{1}{2}\,(E_{j+1} - E_{j-1}) \ , \ j = 2, N - 1 \ , \\ E_N - E_{N-1} \ , \ j = N. \end{cases} \tag{2.2.3}$$

Since $\dot{F}$ is the total energy flux, then the energy flux spectrum $\dot{F}(E_j)$ is

$$\dot{F}(E_j) = \frac{\dot{F}U(E_j)}{\int U(E)\, dE} \approx \frac{\dot{F}U(E_j)}{\sum_{j=1}^{N} U(E_j)\, \Delta E_j} \ . \tag{2.2.4}$$

The number flux spectrum $\dot{N}(E_j)$ is

$$\dot{N}(E_j) = \frac{\dot{F}(E_j)}{E_j} \ , \tag{2.2.5}$$

and the number flux of photons with energies centered about E_j is

$$\dot{n}(E_j) = \dot{N}(E_j)\, \Delta E_j \ . \tag{2.2.6}$$

The incident photon number spectrum $\dot{n}(E_j)$ now must be attenuated through a set of planar shields in front of the cable, and then through the cable itself. It is assumed that exponential attenuation is sufficient to describe the situation; in other words, multiple photon scattering (from Compton scattering) is not important for X-ray spectra of interest (below, say, 300 keV) and neither detailed photon transport has to be taken into account, nor do "buildup factors" have to be included. In brief,

$$\dot{n}(E_j)^{OUT} = \dot{n}(E_j)^{IN} \exp[-\mu(E_j) \text{ x density x g.p.l.}] \tag{2.2.7}$$

where μ is the attenuation coefficient and g.p.l. stands for geometrical path length.

First we discuss planar attenuation and its geometry. We had in mind the fact that cables will rarely be directly exposed to radiation but will be shielded somewhat by a side of a box or the skin of the system, for example. Adding attenuators is also a way of hardening the system. For convenience the plane of the incident radiation is normal to the absorbing plane, but the photon direction itself need not be parallel to the absorbing plane's normal. This is shown in Fig. 2.2.2.

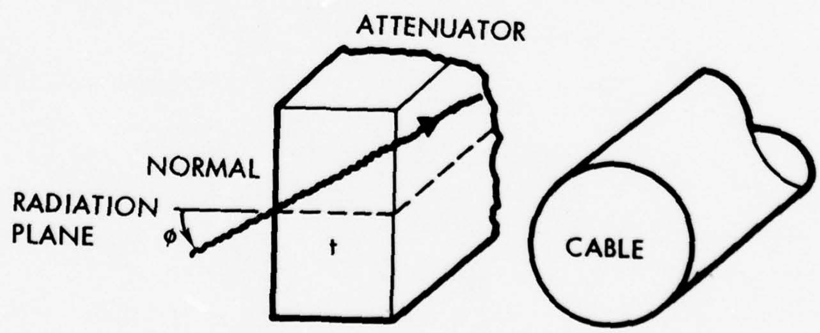

Figure 2.2.2 Planar attenuation of photons before exposure of cable.

The geometrical path length (g.p.l.) is clearly

$$\text{g.p.l.} = t \sec \phi, \tag{2.2.8}$$

where t is the attenuator thickness and ϕ is the angle that the photon direction makes with the attenuator normal ($0 \leq \phi < 90°$).

Next consider the attenuation through the cable itself (Fig. 2.2.3). Let us pick the origin of coordinates as the center of the shield, and the shield axis as the z axis. The photons are considered to be incident in discrete planar sheets, parallel to the x-z plane, and labeled by the coordinate y, the perpendicular distance of the plane to the z axis. The photon's direction in this coordinate system is

$$\vec{n}_{phot} = \vec{i} \cos \phi - \vec{k} \sin \phi , \tag{2.2.9}$$

where ϕ has the same meaning as before in our discussion of planar attenuation. What is the geometrical path length of a photon starting at the point $P_1(x_1,y_1,z_1)$ and arriving at $P_2(x_2 = y_1,z_2)$? Because of the particular choice of axes, $y_2 = y_1$, the projection of the geometrical path length onto the x axis is given by

$$\text{g.p.l.} = \text{projected g.p.l.} \times \sec \phi . \tag{2.2.10}$$

This will be true for any sheet of photons regardless of its coordinate y. The point of this is that we can 1) talk about projected g.p.l.'s exclusively, as if the radiation were normally incident (along the x-axis), and 2) reduce the problem to two dimensions. After calculating the projected g.p.l., we simply have to remember to multiply by sec ϕ.

So now we look at a cross section of a multiconductor cable, as in Fig. 2.2.4. A plane containing the incident photons intersects the cable at coordinate y. The problem of finding the projected path length reduces to 1) finding the x-intersections of the line y with the different interfaces (the dots in the Fig. 2.2.4) and 2) taking the difference between successive intersections. In terms of the notation in the figure, these x-intersections for a fixed y are given by

$$x = \rho \cos \theta \pm \sqrt{\begin{Bmatrix} a^2 \\ b^2 \end{Bmatrix} - [y - \rho \sin \theta]^2} . \tag{2.2.11}$$

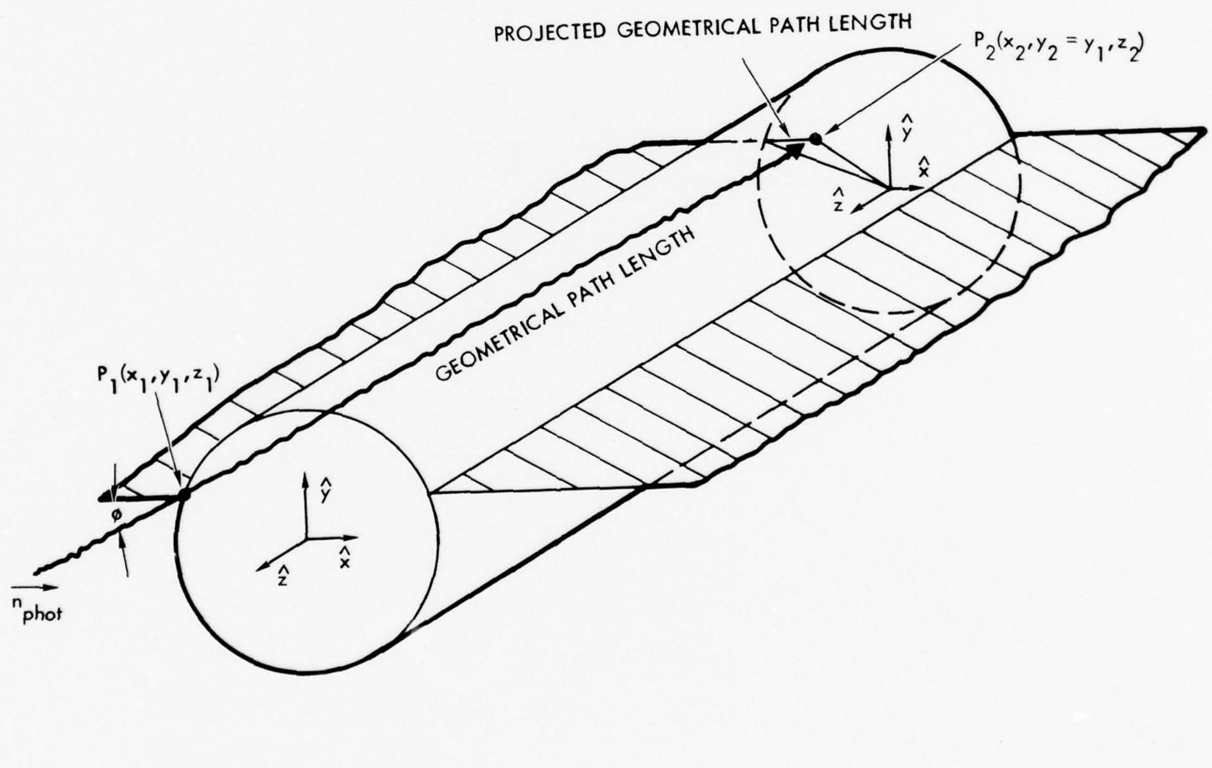

Figure 2.2.3 Attenuation through the cable.

The radius a is to be used for conductor intersections, b for dielectric intersections. (For purposes of calculating attenuation, we ignore gaps). If an intersection is to occur, it occurs in pairs. If the discriminant is negative, no intersection occurs. In summary, we calculate x-intersections via Eq. (2.2.11), calculate the projected path length by taking differences, multiply by sec ϕ to set the full geometrical path length, "remember" what material it is in, look up the appropriate attenuation coefficient, and attenuate the number flux $\dot{n}(E_j)$ to that point via Eq. (2.2.7).

For purposes of calculating electron deposition in the dielectric it is necessary to know the direction cosines of the normal to the conductor at the point where the plane (labeled by y) intersects the conductor at x. Assuming the intersection $\vec{r} \equiv (x,y)$ is known, the conductor normal unit vector satisfies (see Fig. 2.2.4).

$$\vec{n} = \frac{\vec{r} - \vec{\rho}}{a} = \frac{\vec{i}(x - \rho \cos \theta) + \vec{j}(y - \rho \sin \theta)}{a} \equiv \vec{i}\gamma_x + \vec{j}\gamma_y \; , \qquad (2.2.12)$$

which identifies the direction cosines γ_x and γ_y for interior conductors. For the shield the direction cosines are $\gamma_x = -x/a$, $\gamma_y = -y/a$ respectively. The angle that the incident photon makes with the conductor normal is

$$\cos^{-1} \vec{n}_{phot} \cdot \vec{n} = \cos^{-1} (\gamma_x \cos \phi) \; , \qquad (2.2.13)$$

where Eqs. (2.2.9) and (2.2.12) have been used.

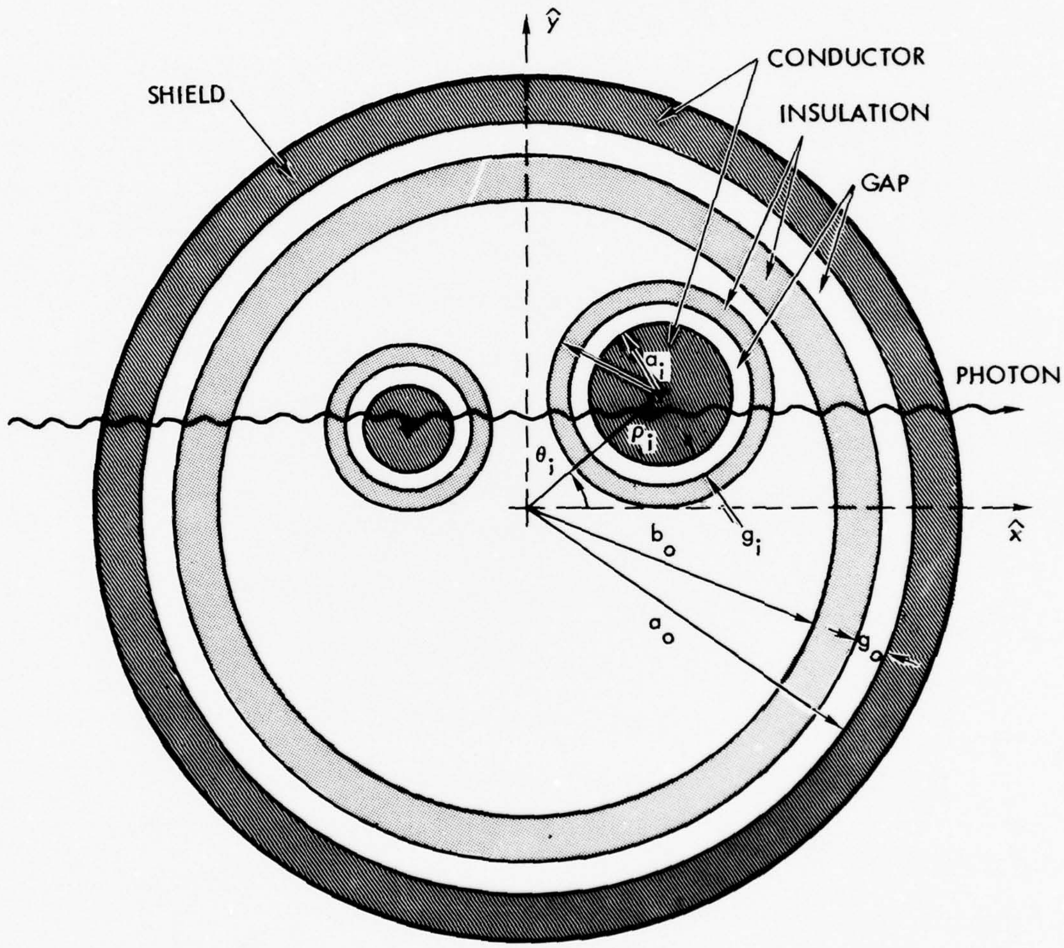

Figure 2.2.4 Cross-section of a multi-conductor cable. Geometric quantities in the figure represent input to the MCCABE code.

2.3 ELECTRON DEPOSITION

To evaluate Eq. (2.1.6) for the Norton drivers we require the emission current from each conductor surface and the deposited charge profile in the dielectric volume. To obtain this we apply the analytic prescriptions given by Dellin and MacCallum[4)] for the case of a planar interface between two semi-infinite media. While the conductor-dielectric interfaces in real cables are not planar, the distance traveled by electrons is usually much smaller than conductor dimensions, and the planar approximation is reasonable.

The first term in the expression for the Norton driver (Eq. 2.1.6) is the charge deposition term involving $\partial q/\partial t$. Since charge deposition occurs in the region surrounding each conductor and does not extend very far into the bulk dielectric, at least for x-rays whose energy is less than 300 keV, it is convenient to break up the volume integration over the entire dielectric into a set of integrations near each conductor surface, i.e.

$$\int d^2r \, \frac{dq}{dt} \, \psi_i \simeq \sum_k \oint d\ell_k \int d\eta \, \frac{dq}{dt} \, \psi_i \tag{2.3.1}$$

Here $d\ell_k$ is a element of arc length about conductor k and η is integrated along the conductor normal from the conductor - dielectric interface into the volume. Dellin and MacCallum have found that the deposition profile exponentially decays away from the interface value, i.e.

$$\frac{dq}{dt} = \sum_{j=1}^{2} \frac{\dot{Q}_{ij}^{(0)2}}{\dot{Q}_{ij}^{(1)}} \exp\left[-\frac{\dot{Q}_{ij}^{(0)}\eta}{\dot{Q}_{ij}^{(1)}}\right] \tag{2.3.2}$$

All quantities in $\dot{Q}_{ij}^{(0)}$ and $\dot{Q}_{ij}^{(1)}$ are obtained from the QUICKE2 code. However, the emission efficienceis J^N, J^F, and J^B which in QUICKE2 have the units electrons/photon, are multiplied by $-|e|\dot{n}$, where $\dot{n}$ is the attenuated number flux of photons in Eq. (2.2.7), and $\dot{Q}_{ij}^{(0)}$ has the units of amps/cm^2. Also, the electron ranges in QUICKE2 which have the units g/cm^2 are converted to cm, and $\dot{Q}_{ij}^{(1)}$ has the units of amps/cm.

The second term in Eq. (2.1.6) is evaluated as

$$\oint d\ell_i \, \vec{J}\cdot\vec{n}_i = -\oint d\ell_i \, J_i^I \tag{2.3.3}$$

where J_i^I is the normal component of the interface current. (The change of sign comes from the fact that J_i^I is directed out of the conductor into the dielectric in contrast to $\vec{n}_i$). J_i^I is easily obtained: the total charge deposition rate is $\dot{Q}_{i1}^{(0)} + \dot{Q}_{i2}^{(0)}$, but this must be equal to the difference between current coming into the volume, i.e., the interface current J_i^I, and the current leaving it, i.e. the net bulk current, J_i^N. We obtain

$$J_i^I = \sum_{j=1}^{2} \dot{Q}_{ij}^{(0)} + J_i^N \qquad (2.3.4)$$

where J_i^N is taken from QUICKE2 data.

The above expressions apply for the case of mono-energetic incident X-rays. For the case of a distributed source, the full Norton drivers must be built up by superposition. The first index i = 1, 2 indicates the medium in which the deposition occurs and the index 1, 2 indicates the medium in which the electrons are created. The numbers 1 and 2 refer to the media traversed first and second by the X-rays. $\dot{Q}_{ij}^{(0)}$ represents the total charge deposition rate in the given region, while $\dot{Q}_{ij}^{(1)}$ is the first moment of it.* Dellin and MacCallum give the following expressions for $Q_{ij}^{(0)}$ and $Q_{ij}^{(1)}$:

$$\dot{Q}_{ij}^{(0)} = \frac{-(-1)^j \, J_j^N \cos\theta \sqrt{\bar{r}_j} - (-1)^{i+j} \, (J_j^F + J_j^B) \sqrt{\bar{r}_1 \bar{r}_2} \sqrt{3}/2}{\sqrt{\bar{r}_1} + \sqrt{\bar{r}_2}} \,, \qquad (2.3.3)$$

$$\dot{Q}_{ij}^{(1)} = \frac{1}{3} \frac{\bar{r}_i R_i(\bar{E}_j)}{\bar{r}_j R_j(\bar{E}_j)} \left\{ \frac{\sqrt{1+1/2\ S_{3-j}}}{\sqrt{1+1/2\ S_1} + \sqrt{1+1/2\ S_2}} \left[R_j(\bar{E}_j)\bar{r}_j (J_j^F + J_j^R) \right.\right.$$

$$\left.\left. - \frac{(-1)^i R_j(\bar{E}_j)\ J_j^N \cos\theta \sqrt{3}/2}{\sqrt{1+1/2\ S_j}} \right] - \delta_{ij}\ R_j(\bar{E}_j)\bar{r}_j (J_j^F + J_j^B, \right\} \qquad (2.3.4)$$

*In general, there are sets of $Q_{ij}^{(0)}$ and $Q_{ij}^{(1)}$ for each electron source type (photo-electric, Auger, Compton), but because of our restruction to photon energies below 300keV where the photo-electric effect dominates, we calculate only one set of the $Q_{ij}^{(0)}$ and $Q_{ij}^{(1)}$.

where

$R_i(E)$ = total electron range in the i^{th} material at energy E,

$\bar{E}_i$ = average energy of electrons created in the i^{th} material,

$\bar{r}_i$ = ratio of mean vector range to total rnage in the i^{th} material,

S_i = $1/\bar{r}_i - 1$,

J_i^N, J_i^F, J_i^B = the net, forward, and back bulk currents in the i^{th} material.

θ = angle between photon direction and interface normal ($\leq 90°$)

2.4 LAPLACE EQUATION IN TWO DIMENSIONS

We present a technique for solving the two-dimensional Laplace equation which takes advantage of the fact that a cross-section of a multiconductor cable shows a collection of arbitrarily placed circles, as in Fig. 2.2.4. Rather than go through the laborious procedure of finite differencing the Laplace equation, we simply write down the formal solution,

$$4\pi\varepsilon_o \phi(\vec{r}) = \sum_{i=1}^{N} a_i \int_o^{2\pi} d\theta' \, \sigma_i(\theta') \, \ell n \, \frac{\frac{r'^2}{a_o^2} \left| \vec{r} - \frac{a_o^2}{r'^2} \vec{r}' \right|^2}{\left| \vec{r} - \vec{r}' \right|^2} , \qquad (2.4.1)$$

where $\vec{r}' = \vec{\rho}_i + \vec{a}_i'$, and $\vec{\rho}_i = (\rho_i, \theta_i)$, $\vec{a}_i' = (a_i, \theta_i')$.

The various geometrical quantities are shown in Fig. 2.2.4. But, in this development, we assume that the dielectric is homogeneous and that there are no gaps. The logarithmic term is seen to be the Green's function for a cylinder of radius a_o which is infinite in length: this guarantees not only that the potential satisfies Laplace's equation, but that it also vanishes on the shield whose radius is a_o. The unknown charge density σ_i on each conductor includes both free and bound charge (free charge density = $K\sigma_i$ where K is the dielectric constant near conductor i). Since we are assuming a homogeneous dielectric, there are no dielectric-dielectric interface charge densities to worry about. (The complication of dielectric interfaces is discussed below). The first step in obtaining the unknown charge densities is to expand Eq. (2.4.1) in circular harmonics (cos nθ', sin nθ');

$$4\pi\varepsilon_o \phi(\vec{r}) = \sum_{i=1}^{N} \sum_{n=o}^{\infty} V_{in}^{+} (\vec{r}) \cdot X_{in}, \qquad (2.4.2)$$

where the spinor V_{in} is given in Appendix B. The spinor X_{in} has replaced the unknown charge densities by a set of unknown coefficients,

$$X_{in} = a_i \int_o^{2\pi} d\theta' \sigma_i(\theta') \begin{bmatrix} \cos n\theta' \\ \sin n\theta' \end{bmatrix}, \qquad (2.4.3)$$

the very first one of which yields exactly the induced free charge per unit length $Q_i = K X_{io}$. The coefficients X are determined by placing the prescribed potentials $V_i = \psi(\vec{\rho} + \vec{a}_i)$, $\vec{a}_i = (a_i, \theta)$, on the boundaries, and multiplying Eq. (2.4.2) by $(4\pi)^{-1}\int_o^{2\pi} d\theta\ (\cos n\theta, \sin n\theta)^+$. This results in the matrix equation

$$2\pi\varepsilon_o\begin{pmatrix}\delta_{no} V_i\\ o\end{pmatrix} = \sum_{i'=1}^{N} \sum_{n'-o}^{\infty} A_{in', i'n'} X_{i'n'} , \qquad (2.4.4)$$

where the matrix A is given in Appendix B. (In practice the infinite sum over n' is truncated). This procedure determines the capacitance matrix as well.

Correction for Non-Homogeneous Dielectric:

Multiconductor cables in practice will not usually have homogeneous dielectrics; contrary to our assumption above, the existence of gaps between insulation and conductors as well as dielectric-dielectric interfaces is the more likely possibility. Our assumption is that non-homogeneities in the dielectric will not affect the capacitance matrix very much (<50%). On the other hand the effect on the potential distribution near conductor-dielectric interfaces is considerable, as will be made clear by the following argument. Consider a parallel plate capacitor whose plate separation is D, but with a small gap d (d<<D) which nonetheless is larger than the range p of an electron penetrating the dielectric. If the dielectric medium were uniform then the potential distribution at $X = d + p \tilde{=} d$, would be $\phi/V = d/D$. However, the presence of a gap (whose dielectric constant was unity) would imply a potential at the same point of $\phi/V = Kd/D$, again assuming d<<D. This suggests that for electrons which cross gaps, we calculate the Laplace solution using the formalism of this section where the dielectric constant is that of the dielectric insulation, and then scale the charge profile by multiplying by K. (In principle, of course one can extend the formalism of the last section by demanding the normal component of the displacement vector to be continuous at the dielectric-dielectric interface. This would introduce a set of dielectric interface charge densities). The $\psi_i(\vec{r})$ in Eq. (2.1.6) are obtained by setting $V_i = 1$ in Eq. (2.4.4) and then using Eq. (2.4.2) to obtain the potential.

3.0 STRUCTURE AND USE OF THE MCCABE CODE

The MCCABE code was written for use on an interactive, time-share computer system. The code itself consists of four separate subprograms, each of which can be run separately. Briefly, these subprograms accomplish the following:

1. FLUXPAK concerns itself with the incident x-ray spectrum and looking up the appropriate photon attenuation coefficients as a function of this energy spectrum.
2. ATTNPAK calculates the photon attenuation of the incident spectrum until it reaches conductor/dielectric interfaces.
3. CIRCLES calculates the capacitance matrix and solves Laplace's equation.
4. DRIVPAK calculates the electron deposition in the dielectric, and the appropriate Laplace equation solutions to obtain the Norton equivalent drivers.

Needless to say, all these subprograms are communicating with each other in a complicated way. Fig. 3.1 gives a flowchart of input and output between the user and the various subprograms. Table 3.1 lists the information contained in each input/output file.

Because of the complicated communication between subprograms we have written the MCHELP code which handles input and program control without the user having to think too much about it. MCHELP is a user-oriented code which interrogates the user and then performs two functions:

1. It constructs all necessary input files from user-supplied data on the cable geometry and x-ray environment.
2. It sets up a job control file for running the various subprograms.

Fig. 3.2 gives an example of a session between user and MCHELP for the case of a simple coax. The explanatory text provided by MCHELP identifies the variables, and their units, as required by MCCABE. The job file (TAPE44) assumes that the various input files (TAPE5, TAPE3, TAPE15) have been given arbitrary file names and stored in memory. Furthermore, it is assumed that relocatable binary versions of FLUXPAK, ATTNPAK, CIRCLES, and DRIVPAK have been stored under the names BFLUX, BATTN, BCIRCL, and BDRIV, respectively. Fig.3.3 gives the job file produced during the session shown in Fig. 3.2. The output, of this MCCABE run is shown in Fig. 3.4. This problem required 12 CPU seconds on a CDC 6600. Fig. 3.5 lists the input files for a sample three-wire multiconductor cable as produced by MCHELP. Fig. 3.6 gives the output of the CIRCLES and DRIVPAK subprograms of MCCABE which contains the calculated capacitance matrix and Norton drivers. This problem required 87 CPU seconds.

Table 3.1 Data files used with MCCABE.

Name	Use
TAPE5	input of X-ray spectrum and of cable materials description
TAPE3	input of cable geometry
TAPE15	input to control Laplace equation solution
TAPE6	output of photon cross sections
TAPE4	output of attenuated photon flux at interfaces
TAPE16	output of checks on coefficients of the potential expansion and capacitance matrix calculation
TAPE24	output of electron transport and Norton driver calculation
TAPE8=NSTAB	photon cross section data for FLUXPAK (binary)
TAPE9	photon cross sections selected for ATTNPAK
TAPE27=DELMAC	photo-Compton current data from QUICKE2 for DRIVPAK
TAPE10	photon flux at conductor/dielectric interface for DRIVPAK
TAPE12	coefficients of potential expansions for DRIVPAK

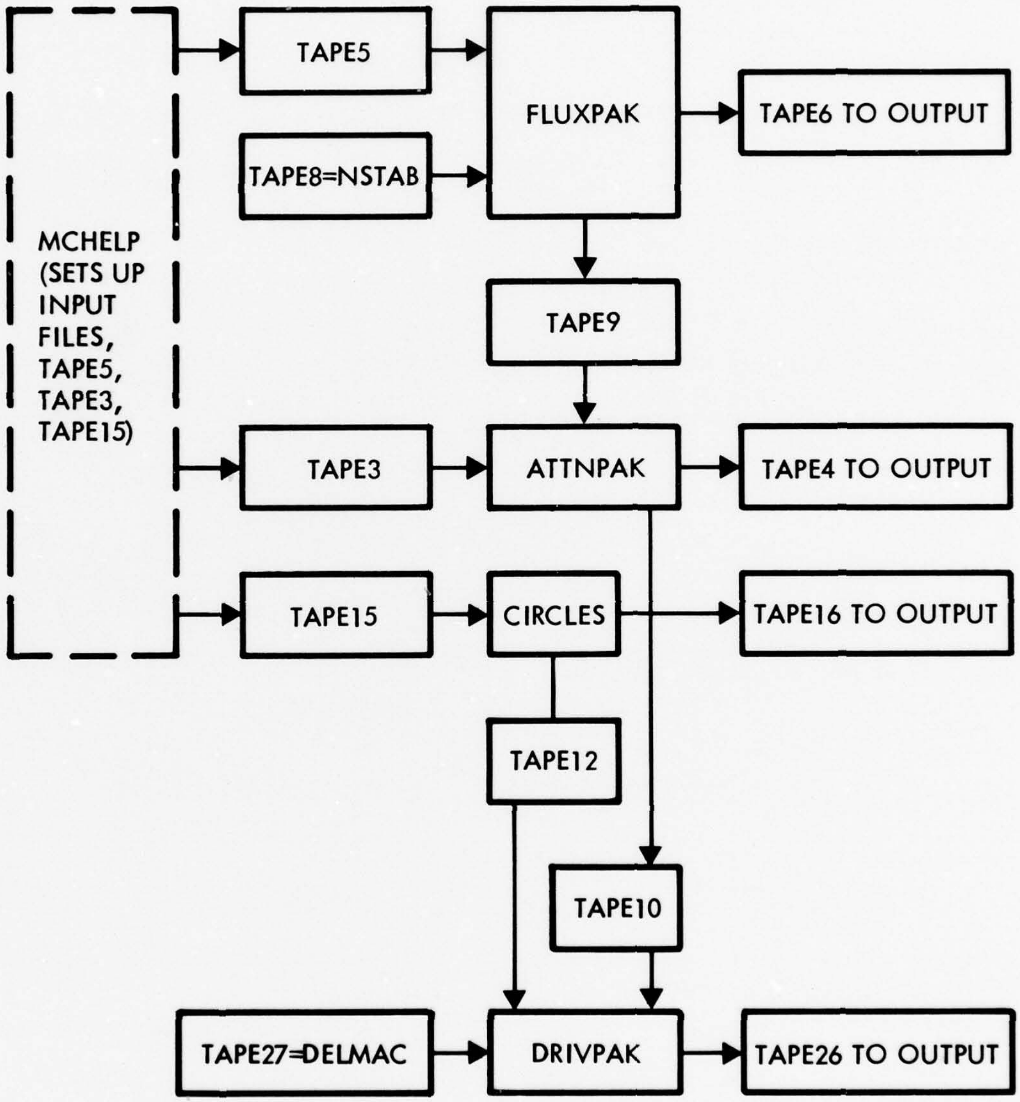

Figure 3.1 Flow-chart of input/output communication among subroutines in MCCABE.

```
MCHELP 8/3/77
THIS CODE SETS UP INPUT INFO FOR THE MCCABE CODE
THE INFO REQUIRED IS DIVIDED INTO 2 PARTS:
 CABLE GEOMETRY AND SPECTRUM
 EXECUTION INSTRUCTIONS

THE OUTPUT OF THIS CODE IS A PERFORM FILE(TAPE44)
AND VARIOUS FILES WHICH MAY BE SAVED



CABLE GEOMETRY AND SPECTRUM

INPUT INFO  WHICH YOU GIVE SHOULD FOLLOW
NAMELIST RULES
WITH END OF ENTRY INDICATED BY $
IF YOU HAVE INFO IN PERM STORAGE
PROVIDE DUMMY INFO OR NONE AT ALL

DO YOU WANT TO CONSTRUCT TAPE5
FOR FLUXPAK? (1=YES,0=NO)
? 1


PHOTON1 NAMELIST
FLUX=FLUX IN CAL/CM2SEC
NMIX= NUMBER OF DISTINCT MATERIALS(MAX=10)
N= NUMBER OF PHOTON ENERGIES (MAX=50)
EPHOT(I),I=1,N ARE PHOTON ENERGIES(KEV)
U(I),I=1,N ARE UNNORM. ENERGY SPECTRA(/KEV)
IF EQUALLY SPACED ENTER EPHOT(1) AND EPHOT(N) ONLY
XKT IS BB TEMP IN KEV(IGNORED IF NOT ENTERED)
PHI  IS ANGLE(DEGREES) BETWEEN SHIELD NORMAL
PROJECTED IN PLANE OF INCIDENT RADIATION
AND DIRECTION  OF INCIDENT RADIATION (<90 DEG)
IPRT=NONZERO  GIVES LONG PRINT


 $PHOTON1
? FLUX=1,N=1,EPHOT=50,U=1,NMIX=4$
YOU WILL BE ASKED  FOR   4

MIXTURE NAMELIST
FOR EACH MATERIAL(OF UP TO 10 COMPONENTS):
THE ORDER OF ENTRY DOES NOT MATTER
BUT THE MATERIAL LABEL INDEX
WHICH FOLLOWS LATER IN THE INPUT CORRESPONDS
TO THIS ORDER OF ENTRY
ZA= Z NUMBERS(IN ORDER OF INCREASING Z)
WT= WEIGHT FRACTIONS
AT=ATOMIC WEIGHT
DENSITY=DENSITY(G/CM3)
IZDM=Z NO. OF ELEMENT OR LABEL NO. IN DELMAC TABLE
```

Note:

Dielectric type	Label No.
water	901
teflon	902
PVC	903
Mylar	904
Kapton	905
Halar	906
Kel-F	907

Figure 3.2 Terminal printout from MCHELP for a simple coax.

```
 $MIXTURE
? ZA=29,AT=63.54,WT=1,DENSITY=8.9,IZDM=29$
 $MIXTURE
? ZA=6,9,AT=12.01,19.,WT=.24,.76,DENSITY=2.2,IZDM=902$
 $MIXTURE
? ZA=50,AT=118.7,WT=1,DENSITY=7.2,IZDM=50$
 $MIXTURE
? ZA=47,AT=107.9,WT=1,DENSITY=10.5,IZDM=47$

 TAPE5 HAS BEEN CONSTRUCTED

 DO YOU WANT TO CONSTRUCT TAPE3 AND TAPE15
 FOR ATTNPAK AND CIRCLES? (1=YES,0=NO)
? 1

 ATTPLN NAMELIST
 NPLANE= NO. OF ATTENUATION PLANES(MAY BE 0)
 T(I),I=1,NPLANE = PLANE THICKNESS IN CM
 IPLANLB, I=1,NPLANE=MIXTURE INDICIES
 WHICH IS THE ORDER IN WHICH MIXTURES WERE READ
  $ATTPLN
? $

 CONDUCT NAMELIST
 ALL DISTANCES IN CM, ANGLES IN DEGREES
 NCON=NO. OF COND'S INCLUDING SHIELD
 TSHIELD=SHIELD THICKNESS
 RADC(I),I=1,NCON ARE COND. RADII
 RADD             ARE DIELECTRIC RADII
 GAP              ARE GAP SIZES
 THE FIRST ENTRY OF RADC,RADD,GAP REFERS TO SHIELD
 MATLBLC(I),I=1,NCON IS THE MATERIAL LABEL INDEX
 MATLBLD(I)             "
 MATLBLF(I)             "
  WHERE C IS THE CONDUCTOR, D DIEL., F FLASHING,
  AND THE LABEL INDEX CORRESPONDS TO
  THE ORDER IN WHICH MIXTURES WERE READ IN ABOVE
 MATBAK IS THE BACKGROUND DIELECTRIC INDEX
 DFLASH(I),I=1,NCON ARE FLASHING THICKNESSES
 RO(I),THET(I),I=1,NCON ARE THE COORDS. OF COND. I
 2 TIMES NY IS THE NO. OF Y PLANES  INTERSECTING SHIELD
 IPRT=NONZERO GIVES LONG PRINT

  $CONDUCT
? NCON=2,RO=0,0,NY=10
? MATLBLC=1,1,MATLBLD=2,2,MATBAK=2
? RADC=.1,.0299
? GAP=.005,.001
? RADD=.0651,.065
? TSHIELD=.01
? MATLBLF=3,4,DFLASH=.0002,.0002$

 TAPE3 HAS BEEN CONSTRUCTED
```

Note: The flashing modification is a phenomenological adjustment of the interface current discussed in Refs. 2 and 7.

```
 INPUT TO CIRCLES AND TAPE15 CONSTRUCTION

 MOST INPUT WAS GIVEN IN ATTNPAK FOR CIRCLES

 PERM NAMELIST
 PER=DIELECTRIC CONSTANT
 MMAX=MAX TERMS IN HARMONIC EXPANSION
 EPSLN TIMES MIN. DIAG ELEMENT IS LARGEST OFF-DIAG

  $PERM
? PER=2.1,MMAX=1$
  TAPE15 HAS BEEN CONSTRUCTED
```

Note: MMAX=1 is sufficient for coaxes. MMAX=4-6 is sufficient for cable bundles depending on degree of assymetry. EPSLN=0 means no off-diagonal matrix elements are discarded before entering sparse matrix routines

Figure 3.2 (continued) Terminal printout from MCHELP for a simple coax.

```
EXECUTION INSTRUCTIONS

 SHOULD FLUXPAK BE EXECUTED
 (1=YES,0=NO)
? 1
 NAME OF TAPE5
? COAX5
 NAME OF TAPE9
? COAX9


 SHOULD ATTNPAK BE EXECUTED
 (1=YES,0=NO)
? 1
 NAME OF TAPE3
? COAX3
 NAME OF TAPE9
? COAX9
 NAME OF TAPE10
? COAX10


 SHOULD CIRCLES BE EXECUTED
 (1=YES,0=NO)
? 1
 NAME OF TAPE15
? COAX15
 NAME OF TAPE12
? COAX12


 SHOULD DRIVPAK BE EXECUTED
 (1=YES,0=NO)
? 1
 NAME OF TAPE10
? COAX10
 NAME OF TAPE12
? COAX12


 FILES CONSTRUCTED:
 TAPE44(PERFORM FILE)
 TAPE5(INPUT FOR FLUXPAK)
 TAPE3(INPUT FOR ATTNPAK)
 TAPE15(INPUT FOR CIRCLES)

 LIST TAPE44 TO SEE NAMES ASSIGNED TO DATA FILES
 REPLACE TAPE5,TAPE3,TAPE15 UNDER THIER NEW NAMES
 THEN: PERFORM,TAPE44
```

Note: These file names are arbitrary.

Figure 3.2 (continued) Terminal printout from MCHELP for a simple coax.

```
GET,TAPE5=COAX5
GET,TAPE8=NSTAB
GET,BFLUX
BFLUX,TAPE6=OUTPUT
REPLACE,TAPE9=COAX9
GET,TAPE3=COAX3
GET,TAPE9=COAX9
GET,BATTN
BATTN,TAPE4=OUTPUT
REPLACE,TAPE10=COAX10
GET,TAPE15=COAX15
GET,BCIRCL
BCIRCL,TAPE16=OUTPUT
REPLACE,TAPE12=COAX12
GET,TAPE10=COAX10
GET,TAPE12=COAX12
GET,TAPE27=DELMAC
GET,BDRIV
BDRIV,TAPE26=OUTPUT
```

Figure 3.3 Job file created by MCCABE for the example given in Figure 3.2.

```
1 FLUXPAK 8/3/77

 NO. OF MIXTURES                     4
 FLUX(CAL/CM2SEC)                   1.00000E+00
 PHI(DEGREES)                       0.
 PHOTONS/CAL                        5.22600E+14
 TOTAL NFLUX(/CM2SEC)               5.22600E+14
 INDEX/NUMBER FLUX(/CM2SEC)
   1   5.23E+14

 MIXTURE NO./Z NO./DENSITY/ATOMIC WT.
    1   2.90E+01   8.90E+00   6.35E+01

 MIXTURE NO./Z NO./DENSITY/ATOMIC WT.
    2   8.28E+00   2.20E+00   1.73E+01

 MIXTURE NO./Z NO./DENSITY/ATOMIC WT.
    3   5.00E+01   7.20E+00   1.19E+02

 MIXTURE NO./Z NO./DENSITY/ATOMIC WT.
    4   4.70E+01   1.05E+01   1.08E+02



1 DRIVPAK 8/3/77


 GEOMETRY VARIABLES TRANSFERRED FROM ATTNPAK
 NCON=         2
 RADC=  1.00E-01  2.99E-02
 GAP=  5.00E-03  1.00E-03
 RADD=  6.51E-02  6.50E-02
 RO=  0.         1.00E-07
 THET=  0.         0.
 MATLBLC=          1          1
 MATLBLD=          2          2
 MATLBLF=          3          4
 DFLASH=  2.00E-04  2.00E-04

 PHOTON ENERGIES
 NE=          1
 EPHOT=  5.00E+01

 TOTAL EMITTED CURRENT FROM SHIELD AND EACH CONDUCTOR
 ISURF=  8.36E-08  2.40E-08

 TOTAL INDUCED CURRENT ON EACH CONDUCTOR  DUE TO DEPOSITED CHARGE
 IAREA= -2.97E-08

 NORTON DRIVER TO EACH CONDUCTOR(SHORT CIRCUIT CURRENT) (A/CM)
 ISC= -5.67E-09
```

Figure 3.4 MCCABE output for the coax defined in Figure 3.2.

```
1 ATTNPAK 8/3/77

 X/Y/X DIR/YDIR/ANGLE/CON NO.
 ENERGY BIN/NO. FLUX UNIT LENEGTH
 -3.12E-02 -9.50E-02  3.12E-01  9.50E-01  1.25E+00   1
   1  2.78E+13
  3.12E-02 -9.50E-02 -3.12E-01  9.50E-01  1.89E+00   1
   1  2.71E+13
 -5.27E-02 -8.50E-02  5.27E-01  8.50E-01  1.02E+00   1
   1  1.38E+13
  5.27E-02 -8.50E-02 -5.27E-01  8.50E-01  2.13E+00   1
   1  1.33E+13
 -6.61E-02 -7.50E-02  6.61E-01  7.50E-01  8.48E-01   1
   1  1.16E+13
  6.61E-02 -7.50E-02 -6.61E-01  7.50E-01  2.29E+00   1
   1  1.10E+13
 -7.60E-02 -6.50E-02  7.60E-01  6.50E-01  7.08E-01   1
   1  1.04E+13
  7.60E-02 -6.50E-02 -7.60E-01  6.50E-01  2.43E+00   1
   1  9.81E+12
 -8.35E-02 -5.50E-02  8.35E-01  5.50E-01  5.82E-01   1
   1  9.70E+12
  8.35E-02 -5.50E-02 -8.35E-01  5.50E-01  2.56E+00   1
   1  9.06E+12
 -8.93E-02 -4.50E-02  8.93E-01  4.50E-01  4.67E-01   1
   1  9.20E+12
  8.93E-02 -4.50E-02 -8.93E-01  4.50E-01  2.67E+00   1
   1  8.55E+12
 -9.37E-02 -3.50E-02  9.37E-01  3.50E-01  3.58E-01   1
   1  8.86E+12
  9.37E-02 -3.50E-02 -9.37E-01  3.50E-01  2.78E+00   1
   1  8.20E+12
 -9.68E-02 -2.50E-02  9.68E-01  2.50E-01  2.53E-01   1
   1  8.63E+12
 -1.64E-02 -2.50E-02 -5.49E-01 -8.36E-01  2.15E+00   2
   1  2.02E+13
  1.64E-02 -2.50E-02  5.49E-01 -8.36E-01  9.90E-01   2
   1  9.90E+12
  9.68E-02 -2.50E-02 -9.68E-01  2.50E-01  2.89E+00   1
   1  3.95E+12
 -9.89E-02 -1.50E-02  9.89E-01  1.50E-01  1.51E-01   1
   1  8.49E+12
 -2.59E-02 -1.50E-02 -8.65E-01 -5.02E-01  2.62E+00   2
   1  9.53E+12
  2.59E-02 -1.50E-02  8.65E-01 -5.02E-01  5.26E-01   2
   1  3.09E+12
  9.89E-02 -1.50E-02 -9.89E-01  1.50E-01  2.99E+00   1
   1  2.59E+12
 -9.99E-02 -5.00E-03  9.99E-01  5.00E-02  5.00E-02   1
   1  8.42E+12
 -2.95E-02 -5.00E-03 -9.86E-01 -1.67E-01  2.97E+00   2
   1  8.32E+12
  2.95E-02 -5.00E-03  9.86E-01 -1.67E-01  1.68E-01   2
   1  2.30E+12
  9.99E-02 -5.00E-03 -9.99E-01  5.00E-02  3.09E+00   1
   1  2.20E+12
```

Figure 3.4 (continued) MCCABE output for the coax defined in Figure 3.2

```
1$PHOTON1
 FLUX    = 1.0,
 N       = 1,
 EPHOT   = 5.0E+01, 0., 0., 0., 0., 0., 0., 0., 0., 0., 0., 0., 0., 0.,
+ 0., 0., 0., 0., 0., 0., 0., 0., 0.,
           0., 0., 0., 0., 0., 0., 0., 0., 0., 0., 0., 0., 0., 0., 0., 0
+ ., 0., 0., 0., 0., 0., 0., 0., 0., 0.,
           0., 0.,
 U       = 1.0, 0., 0., 0., 0., 0., 0., 0., 0., 0., 0., 0., 0., 0., 0.,
+ 0., 0., 0., 0., 0., 0., 0., 0., 0.,
           0., 0., 0., 0., 0., 0., 0., 0., 0., 0., 0., 0., 0., 0., 0., 0
+ ., 0., 0., 0., 0., 0., 0., 0., 0., 0.,
           0.,
 NMIX    = 4,
 PHI     = 0.,
 XKT     = 0.,
 IPRT    = 0,
 $END
1$MIXTURE
 ZA      = 2.9E+01, 0., 0., 0., 0., 0., 0., 0., 0., 0.,
 WT      = 1.0, 0., 0., 0., 0., 0., 0., 0., 0., 0.,
 AT      = 6.354E+01, 0., 0., 0., 0., 0., 0., 0., 0., 0.,
 DENSITY = 8.9,
 IZDM    = 29,
 $END
1$MIXTURE
 ZA      = 1.0, 6.0, 7.0, 8.0, 0., 0., 0., 0., 0., 0.,
 WT      = 9.41E-03, 5.6091E-01, 1.3082E-01, 2.9886E-01, 0., 0., 0., 0.,
+  0., 0.,
 AT      = 1.0, 1.2E+01, 1.4E+01, 1.6E+01, 0., 0., 0., 0., 0., 0.,
 DENSITY = 1.42,
 IZDM    = 905,
 $END
1$MIXTURE
 ZA      = 5.0E+01, 0., 0., 0., 0., 0., 0., 0., 0., 0.,
 WT      = 1.0, 0., 0., 0., 0., 0., 0., 0., 0., 0.,
 AT      = 1.187E+02, 0., 0., 0., 0., 0., 0., 0., 0., 0.,
 DENSITY = 7.2,
 IZDM    = 50,
 $END
1$MIXTURE
 ZA      = 4.7E+01, 0., 0., 0., 0., 0., 0., 0., 0., 0.,
 WT      = 1.0, 0., 0., 0., 0., 0., 0., 0., 0., 0.,
 AT      = 1.079E+02, 0., 0., 0., 0., 0., 0., 0., 0., 0.,
 DENSITY = 1.05E+01,
 IZDM    = 47,
 $END
```

Figure 3.5 (a) Input file, TAPE5, for MCCABE created by MCHELP for a 3-wire multi-conductor cable.

```
1$ATTPLN
 NPLANE   = 0,
 T        = 0., 0., 0., 0., 0., 0., 0., 0., 0., 0., 0., 0., 0., 0., 0., 0
+ ., 0., 0., 0., 0.,
 IPLANLB = 0, 0, 0, 0, 0, 0, 0, 0, 0, 0, 0, 0, 0, 0, 0, 0, 0, 0, 0, 0,
 $END
1$CONDUCT
 RADC     = 1.8E-01, 5.0E-02, 5.0E-02, 5.0E-02, 0., 0., 0., 0., 0., 0., 0
+ ., 0., 0., 0., 0., 0., 0., 0., 0., 0.,
            0.,
 RADD     = 1.50001E-01, 6.95E-02, 6.95E-02, 6.95E-02, 0., 0., 0., 0., 0.
+ , 0., 0., 0., 0., 0., 0., 0., 0., 0.,
            0., 0., 0.,
 RO       = 0., 8.03E-02, 8.03E-02, 8.03E-02, 0., 0., 0., 0., 0., 0., 0.,
+  0., 0., 0., 0., 0., 0., 0., 0., 0.,
            0.,
 THET     = 0., 6.0E+01, 1.8E+02, 3.0E+02, 0., 0., 0., 0., 0., 0., 0.
+ , 0., 0., 0., 0., 0., 0., 0., 0., 0.,
 GAP      = 5.0E-03, 1.0E-08, 1.0E-08, 1.0E-08, 0., 0., 0., 0., 0., 0., 0
+ ., 0., 0., 0., 0., 0., 0., 0., 0.,
            0.,
 NCON     = 4,
 TSHIELD = 3.3E-02,
 MATLBLC = 1, 1, 1, 1, 0, 0, 0, 0, 0, 0, 0, 0, 0, 0, 0, 0, 0, 0, 0, 0
+ ,
 MATLBLD = 2, 2, 2, 2, 0, 0, 0, 0, 0, 0, 0, 0, 0, 0, 0, 0, 0, 0, 0, 0
+ ,
 NY       =10,
 MATBAK  = 0,
 MATLBLF =3,4,4,4,
 DFLASH=4*2.E-4,
 IPRT     = 0,
 $END
```

Figure 3.5 (b) Input file, TAPE3, for MCCABE created by MCHELP for a 3-wire multi-conductor cable.

```
1$NAME1
 A        = 5.0E-02, 5.0E-02, 5.0E-02, 0., 0., 0., 0., 0., 0., 0., 0., 0.
+ , 0., 0., 0., 0., 0., 0., 0., 0.,
 B        = 1.8E-01,
 RH       = 8.03E-02, 8.03E-02, 8.03E-02, 0., 0., 0., 0., 0., 0., 0., 0.,
+  0., 0., 0., 0., 0., 0., 0., 0., 0.,
 NMAX     = 3,
 MMAX     = 4,
 PER      = 3.5,
 EPSLN    = 0,
 TH       = 6.0E+01, 1.8E+02, 3.0E+02, 0., 0., 0., 0., 0., 0., 0., 0., 0.
+ , 0., 0., 0., 0., 0., 0., 0.,
 IPRT     = 0,
 $END
```

Figure 3.5 (c) Input file, TAPE15, for MCCABE created by MCHELP for a 3-wire multiconductor cable.

```
1 CIRCLES 8/3/77

 MINIMUM DIAGONAL    1.24996E-01

 CAPACITANCE MATRIX(F/CM)
    1     1     1.33434E-12
    1     2     5.80652E-13
    1     3     5.80652E-13
    2     1     5.80652E-13
    2     2     1.33434E-12
    2     3     5.80652E-13
    3     1     5.80652E-13
    3     2     5.80652E-13
    3     3     1.33434E-12


1 DRIVPAK 8/3/77


 GEOMETRY VARIABLES TRANSFERRED FROM ATTNPAK
 NCON=         4
 RADC=  1.80E-01  5.00E-02  5.00E-02  5.00E-02
 GAP=  5.00E-03  1.00E-08  1.00E-08  1.00E-08
 RADD=  1.50E-01  6.95E-02  6.95E-02  6.95E-02
 RO=  0.         8.03E-02  8.03E-02  8.03E-02
 THET=  0.         6.00E+01  1.80E+02  3.00E+02
 MATLBLC=          1         1         1         1
 MATLBLD=          2         2         2         2
 MATLBLF=          3         4         4         4
 DFLASH=  2.00E-04  2.00E-04  2.00E-04  2.00E-04

 PHOTON ENERGIES
 NE=           1
 EPHOT=  5.00E+01

 TOTAL EMITTED CURRENT FROM SHIELD AND EACH CONDUCTOR
 ISURF=  6.34E-08  1.38E-08  2.20E-08  1.38E-08

 TOTAL INDUCED CURRENT ON EACH CONDUCTOR  DUE TO DEPOSITED CHARGE
 IAREA= -1.73E-08 -2.99E-08 -1.73E-08

 NORTON DRIVER TO EACH CONDUCTOR(SHORT CIRCUIT CURRENT) (A/CM)
 ISC= -3.44E-09 -7.89E-09 -3.44E-09
```

Figure 3.6   MCCABE output for the three-wire problem defined in Figure 3.5.

REFERENCES

1. D. M. Clement, C. E. Wuller, and E. P. Chivington, "Multiconductor Cable Response in X-Ray Environments," IEEE Trans. Nucl. Sci. NS-23, 1946 (1976).

2. D. M. Clement and C. E. Wuller, "Assessment of Cable Response Sensitivity to Cable and Source Parameters in Low Fluence X-Ray Environments," Defense Nuclear Agency DNA-4407T, 8 April 1977.

3. C. E. Wuller, L. C. Nielsen, and D. M. Clement, "Definition of the Linear Region of X-Ray Induced Cable Response," Defense Nuclear Agency DNA 4405T, 13 May 1977.

4. T. A. Dellin and C. J. MacCallum, "Analytical Photo-Compton Deposition Profiles," IEEE Trans. Nucl. Sci. NS-23, 1866 (1976).

5. T. A. Dellin and C. J. MacCallum, "A Handbook of Photo-Compton Current Data," Sandia Laboratories, SCL-RR-720086, December 1972.

6. T. A. Dellin and C. J. MacCallum, "QUICKE2: A One-Dimensional Code for Calculating Bulk and Vacuum Emitted Photo-Compton Currents," Sandia Laboratories, SLL-74-0218, April 1974.

7. F. Hai, P. A. Beemer, C. E. Wuller, and D. M. Clement, "Measured and Predicted Radiation-Induced Currents in Semirigid Coaxial Cables," IEEE Trans, Nucl. Sci. NS-24, (1977), No. 6.

8. D. M. Clement, L. C. Nielsen, T. J. Sheppard and C. E. Wuller, "Stored Charge Release in Cables in Low Fluence X-ray Environments," IEEE Trans. Nucl. Sci. NS-24, (1977), No. 6.

9. R. L. Fitzwilson, M. J. Bernstein and T. E. Alston, "Radiation Induced Currents in Shielded Multi-Conductor and Semi-rigid Cables," IEEE Trans. Nucl. Sci., NS-21, 276 (1974).

APPENDIX A

REVIEW OF POTENTIAL THEORY

Consider a set of N+1 parallel conductors, the first of which is grounded, separated by a various homogeneous dielectrics. A volume charge density $\rho(\vec{r})$ is deposited in the dielectric at the points $\vec{r}'$. The potential ϕ, the solution of Poisson's equation, and the Green function G satisfy the following: ϕ, G, $K_{\vec{r}} \frac{\partial \phi}{\partial n}$ and $K_{\vec{r}} \frac{\partial G}{\partial n}$ are continuous, G=0 on the conductor boundaries, and

$$\nabla^2 \phi = - \frac{\rho}{\varepsilon_o K_{\vec{r}}} \; , \; \nabla^2 G = - \frac{\delta(\vec{r} - \vec{r}')}{\varepsilon_o K_{\vec{r}}} \; , \tag{A.1}$$

where $\varepsilon_o K_{\vec{r}}$ is the dielectric constant at the point $\vec{r}$. From Green's theorem,

$$\int d^2 r \left(\phi \nabla^2 K_{\vec{r}} G - K_{\vec{r}} G \nabla^2 \phi \right) = \int ds \left(\phi \frac{\partial}{\partial n} K_{\vec{r}} G - K_{\vec{r}} G \frac{\partial \phi}{\partial n} \right) \tag{A.2}$$

we obtain a representation for ϕ,

$$\phi(\vec{r}) = \int d^2 r' \rho(\vec{r}') G(\vec{r}' \vec{r}) - \varepsilon_o \sum_{j=1}^{N+1} V_j \int ds_j \, K_{\vec{r}_j} \frac{\partial G(\vec{r}_j \vec{r})}{\partial n_j} \; , \tag{A.3}$$

where V_j is the potential of the j^{th} conductor. The normal $\vec{n}_j$ at the surface whose incremental line element is ds_j, is directed out of the dielectric volume. A second application of Green's theorem (with G replacing ϕ in Eq. (A.2)) establishes a symmetry of G,

$$G(\vec{r}\vec{r}') = G(\vec{r}'\vec{r}). \tag{A.4}$$

The induced charge on conductor i is

$$Q_i = \varepsilon_o \int ds_i K_{\vec{r}_i} \frac{\partial \phi}{\partial n_i}$$

$$= \varepsilon_o \int ds_i K_{\vec{r}_i} \int d^2 r' \rho(\vec{r}') \frac{\partial G}{\partial n_i} (\vec{r}' \vec{r})$$

$$- \varepsilon_o^2 \sum_{j=1}^{N} V_j \int ds_i \frac{\partial}{\partial n_i} K_{\vec{r}_i} \int ds_j \frac{\partial}{\partial n_j} K_{\vec{r}_j} G(\vec{r}_j \vec{r}_i) \quad . \tag{A.5}$$

We proceed to simplify the interpretation of Eq. (A.5). First we define the capacitance matrix

$$k_{ij} = - \varepsilon_o^2 \int ds_i \frac{\partial}{\partial n_i} K_{\vec{r}_i} \int ds_j K_{\vec{r}_j} \frac{\partial}{\partial n_j} G(\vec{r}_j \vec{r}_i). \tag{A.6}$$

Next, considered Eq. (A.3) with $\rho = 0$, and with all conductors grounded except conductor i which has unit potential. The potential at the point $\vec{r}'$, which we now call $\psi_i(\vec{r}')$, satisfies

$$\psi_i(\vec{r}') = - \frac{1}{\varepsilon_o} \int ds_i K_{\vec{r}_i} \frac{\partial}{\partial n_i} G(\vec{r}_i \vec{r}_o). \tag{A.7}$$

This can be inserted into Eq.(A.5) and we have

$$Q_i = - \int d^2 r' \rho(\vec{r}') \psi_i(\vec{r}') + \sum_{j=1}^{N} k_{ij} V_j. \tag{A.8}$$

The first term represents the induced charge, the second the capacitive charge, for the elemental length of cable.

APPENDIX B:

EXPLICIT EXPRESSIONS INVOLVED IN LAPLACE SOLUTION

The vectors $\vec{r} = r, \phi$ and $\vec{\rho}_i = \rho_i \theta_i$ have the shield center as origin; $\vec{r}$ is an arbitrary point at which the potential is evaluated, $\vec{\rho}_i$ is the location of the ith conductor's center with respect to the origin. Define

$$S = \frac{r^2 \rho_i^2}{a_o^2} + a_o^2 - 2\, r\rho_i \cos(\phi - \theta_i),$$

$$T = r^2 + \rho_i^2 - 2r\rho_i \cos(\phi - \theta_i),$$

$$U = \arctan \frac{r\sin\phi - \rho_i \sin\theta_i}{r\cos\phi - \rho_i \cos\theta_i} \, .$$

Then

$$V_{in}(\vec{r}) = \begin{cases} \ln S/T, \; n=0 \\ \dfrac{2}{n}\left(\dfrac{a_i}{\sqrt{T}}\right)^{n'} \begin{bmatrix} \cos(nU) \\ \sin(nU) \end{bmatrix} - \\ - 2 \displaystyle\sum_{m=n}^{\infty} \frac{1}{m} \binom{m}{n} \left(\frac{r\rho_i}{a_o^2}\right)^m \left(\frac{a_i}{\rho_i}\right)^n \begin{bmatrix} \cos([m-n']\,\theta_i - m\phi) \\ -\sin([m-n']\,\phi_i - m\phi) \end{bmatrix}, \; n \neq 0 \end{cases}$$

Replacing $\vec{r} \to \vec{\rho}_i$ and $\vec{\rho}_i \to \vec{\rho}_{i'}$, in S, T and U above, we have for $A_{in,i'n'}$

where $n=0$, $n'=0$

$$A_{in,i'n'} = \delta_{ii'} \ln \frac{a_o^2 - \rho_i^2}{a_i a_o} + (1 - \delta_{ii'}) \ln \frac{S}{T} \, ;$$

where $n>0$, $n'=0$,

$$A_{in,i'n'} = \frac{1}{2} \sum_{n_1=n}^{\infty} \frac{1}{n_1} \binom{n_1}{n} \left(\frac{\rho_i \rho_{i'}}{a_o^2}\right)^{n_1} \left(\frac{a_i}{\rho_i}\right)^n \begin{bmatrix} -\cos ([n_1-n]\ \theta_i - n_i \theta_{i'}) \\ \sin ([n_1-n]\ \theta_i - n_i \theta_{i'}) \end{bmatrix}$$

$$+ \frac{1}{2n} (1 - \delta_{ii'}) \left(\frac{a_i}{\sqrt{T}}\right)^n \begin{bmatrix} \cos (nU) \\ \sin (nU) \end{bmatrix} \quad ;$$

and where $n'>0$,

$$A_{in,i'n'} = \frac{(1 - \delta_{ii'})(1 + \delta_{no})}{2n} \binom{-n'}{n} \left(\frac{a_i}{\sqrt{T}}\right)^n \left(\frac{a_{i'}}{\sqrt{T}}\right)^{n'} \begin{bmatrix} \cos ([n+n']\ U), & \sin ([n+n']\ U) \\ \sin ([n+n']\ U), & -\cos ([n+n']\ U) \end{bmatrix}$$

$$+ \frac{1}{2n'} \delta_{nn'} \delta_{ii} \begin{bmatrix} 1, & 0 \\ 0, & 1 \end{bmatrix} - \frac{1}{2} (1 + \delta_{no}) \left(\frac{a_{i'}}{\rho_{i'}}\right)^{n'} \sum_{m=n'}^{\infty} \frac{1}{m} \binom{m}{n'} \left(\frac{\rho_i \rho_{i'}}{a_o^2}\right)^m \binom{m}{n} \left(\frac{a_i}{\rho_i}\right)^n \times$$

$$\times \begin{bmatrix} \cos ([m-n']\ \theta_{i'} - [m-n]\ \theta_i), & -\sin ([m-n']\ \theta_{i'} - [m-n]\ \theta_i) \\ \sin ([m-n']\ \theta_{i'} - [m-n]\ \theta_i), & \cos ([m-n']\ \theta_{i'} - [m-n]\ \theta_i) \end{bmatrix} .$$

The coefficient $\binom{\alpha}{n}$ is defined as

$$\binom{\alpha}{n} = \begin{cases} 0 & , n<0 \\ 1 & , n=0 \\ \dfrac{\alpha(\alpha-1)\ (\alpha-2)\ .\ .\ .\ (\alpha-[n-1])}{n!} & , n>0 \end{cases}$$

DISTRIBUTION LIST

DEPARTMENT OF DEFENSE

Assistant to the Secretary of Defense
Atomic Energy
ATTN: Executive Assistant

Defense Documentation Center
12 cy ATTN: DD

Defense Intelligence Agency
ATTN: DB-4C

Defense Nuclear Agency
ATTN: DDST
2 cy ATTN: RAEV
4 cy ATTN: TITL

Field Command,
Defense Nuclear Agency
ATTN: FCPR
ATTN: FCLMC

Interservice Nuclear Weapons School
ATTN: TTV

Joint Chiefs of Staff
ATTN: J-3, WWMCCS Evaluation Office
ATTN: J-5, Nuclear Division

Joint Strat. Tgt. Planning Staff
ATTN: JLTW-2

Livermore Division, Fld. Command, DNA
Department of Defense
Lawrence Livermore Laboratory
ATTN: FCPRL

National Communications System
Office of the Manager
Department of Defense
ATTN: NCS-TS

Under Secy. of Def. for Rsch. & Engrg.
Department of Defense
ATTN: Strategic & Space Systems (OS)

DEPARTMENT OF THE ARMY

BMD Advanced Technology Center
Huntsville Office
Department of the Army
ATTN: ATC-O

BMD Systems Command
Department of the Army
ATTN: BDMSC-H

Deputy Chief of Staff for Rsch., Dev. & Acq.
Department of the Army
ATTN: DAMA-CSS-N

ERADCOM Technical Support Activity
Department of the Army
ATTN: DRSEL

DEPARTMENT OF THE ARMY (Continued)

Harry Diamond Laboratories
Department of the Army
ATTN: DELHD-N-RCC, R. Gilbert
ATTN: DELHD-N-TI, Technical Library
ATTN: DELHD-N-RBA, J. Rosado
ATTN: DELHD-N-NP

Redstone Scientific Information Ctr.
U.S. Army R&D Command
ATTN: Chief, Documents

U.S. Army Communications Sys. Agency
ATTN: CCM-AD-LB, Library

U.S. Army Foreign Science & Tech. Ctr.
ATTN: DRXST-IS-1

DEPARTMENT OF THE NAVY

Naval Research Laboratory
ATTN: Code 7550, J. Davis
ATTN: Code 6701

Naval Surface Weapons Center
ATTN: Code F31

Office of Naval Research
ATTN: Code 427, H. Mullaney

Strategic Systems Project Office
Department of the Navy
ATTN: NSP

DEPARTMENT OF THE AIR FORCE

Air Force Geophysics Laboratory
ATTN: C. Pike

Air Force Weapons Laboratory
ATTN: SUL
ATTN: NT
2 cy ATTN: DYC
2 cy ATTN: NXS

Deputy Chief of Staff
Research, Development, & Acq.
Department of the Air Force
ATTN: AFRDQSM

Rome Air Development Center, AFSC
ATTN: ESR, E. Burke

Space & Missile Systems Organization/DY
Air Force Systems Command
ATTN: DYS

Space & Missile Systems Organization/MN
Air Force Systems Command
ATTN: MNNG
ATTN: MNNH

DEPARTMENT OF THE AIR FORCE (Continued)

Space & Missile Systems Organization/SK
Air Force Systems Command
ATTN: SKF

Strategic Air Command/XPFS
Department of the Air Force
ATTN: NRI-STINFO, Library
ATTN: XPFS

OTHER GOVERNMENT AGENCIES

NASA
Lewis Research Center
ATTN: N. Stevens
ATTN: C. Purvis
ATTN: Library

DEPARTMENT OF DEFENSE CONTRACTORS

Aerospace Corp.
ATTN: F. Hai
ATTN: J. Reinheimer
ATTN: V. Josephson
ATTN: Library

Avco Research & Systems Group
ATTN: A830, Library

Boeing Co.
ATTN: P. Geren

University of California at San Diego
ATTN: S. De Forest

Computer Sciences Corp.
ATTN: A. Schiff

Dikewood Industries, Inc.
ATTN: Tech. Lib.

Dikewood Industries, Inc.
ATTN: K. Lee

EG&G Washington Analytical Services Center, Inc.
ATTN: Library

Eugene P. Deplomb
ATTN: E. Deplomb

Ford Aerospace & Communications Corp.
ATTN: Technical Library
ATTN: MS G30, D. McMorrow

General Electric Co.
Space Division
ATTN: VFSC, Rm. 4230M, J. Peden

General Electric Company-TEMPO
Center for Advanced Studies
ATTN: DASIAC
ATTN: W. McNamara

Hughes Aircraft Co.
ATTN: Technical Library

DEPARTMENT OF DEFENSE CONTRACTORS (Continued)

Hughes Aircraft Co.
El Segundo Site
ATTN: MS A1080, W. Scott
ATTN: MS A620, E. Smith

Institute for Defense Analyses
ATTN: Classified Library

IRT Corp.
ATTN: Library
ATTN: D. Swift

JAYCOR
ATTN: E. Wenaas
ATTN: Library

JAYCOR
ATTN: R. Sullivan

Johns Hopkins University
Applied Physics Lab.
ATTN: P. Partridge

Kaman Sciences Corp.
ATTN: J. Lubell
ATTN: W. Rich
ATTN: Library

Lawrence Livermore Laboratory
University of California
ATTN: Doc. Con. for Technical Information Dept.
Library

Lockheed Missiles & Space Co., Inc.
ATTN: Dept. 85-85

Los Alamos Scientific Laboratory
ATTN: Doc. Con. for Reports Library

McDonnell Douglas Corp.
ATTN: S. Schneider

Mission Research Corp.
ATTN: R. Stettner
ATTN: C. Longmire

Mission Research Corp.-San Diego
ATTN: Library
ATTN: V. Van Lint

R & D Associates
ATTN: L. Schlessinger
ATTN: C. MacDonald
ATTN: Technical Information Center

Rockwell International Corp.
ATTN: Library

Sandia Laboratories
Livermore Laboratory
ATTN: Doc. Con. for T. Dellin

Sandia Laboratories
ATTN: Doc. Con. for 3141

DEPARTMENT OF DEFENSE CONTRACTORS (Continued)

Science Applications, Inc.
ATTN: W. Chadsey

Spire Corp.
ATTN: R. Little

SRI International
ATTN: Library

DEPARTMENT OF DEFENSE CONTRACTORS (Continued)

Systems, Science & Software, Inc.
ATTN: A. Wilson
ATTN: Library

TRW Defense & Space Sys. Group
ATTN: E. Chivington
ATTN: Technical Information Center
ATTN: D. Clement
ATTN: C. Wuller